An Enhancer Composed of Interlocking Submodules Controls Transcriptional Autoregulation of *Suppressor of Hairless*

Feng Liu[1,2] and James W. Posakony[1,*]
[1]Division of Biological Sciences/CDB, University of California San Diego, 9500 Gilman Drive, La Jolla, CA 92093, USA
[2]Present address: Laboratory of Molecular Pathology, Ludwig Institute for Cancer Research - San Diego Branch, La Jolla, CA 92093, USA
*Correspondence: jposakony@ucsd.edu
http://dx.doi.org/10.1016/j.devcel.2014.02.005

SUMMARY

Positive autoregulation is an effective mechanism for the long-term maintenance of a transcription factor's expression. This strategy is widely deployed in cell lineages, where the autoregulatory factor controls the activity of a battery of genes that constitute the differentiation program of a postmitotic cell type. In *Drosophila*, the Notch pathway transcription factor Suppressor of Hairless activates its own expression, specifically in the socket cell of external sensory organs, via an autoregulatory enhancer called the ASE. Here, we show that the ASE is composed of several enhancer submodules, each of which can independently initiate weak *Su(H)* autoregulation. Cross-activation by these submodules is critical to ensure that Su(H) rises above a threshold level necessary to activate a maintenance submodule, which then sustains long-term *Su(H)* autoregulation. Our study reveals the use of interlinked positive-feedback loops to control autoregulation dynamically and provides mechanistic insight into initiation, establishment, and maintenance of the autoregulatory state.

INTRODUCTION

Positive autoregulation by a gene encoding a DNA-binding transcription factor is a widely utilized mechanism for insuring the long-term maintenance of the factor's expression, well after the signals and other factors that initiated this activity are no longer present (Crews and Pearson, 2009; Hobert, 2011b). One common setting in which such prolonged, stable expression of a transcription factor may be especially advantageous is a postmitotic, differentiated cell type. Here, the autoregulatory factor can function as a "terminal selector," responsible for driving the coexpression of a battery of downstream genes that constitute the cell's differentiation program (Hobert, 2011a).

Suppressor of Hairless (Su(H)) is an ancient, highly conserved protein that acts as the transducing transcription factor for the Notch cell-cell signaling pathway (Fortini and Artavanis-Tsakonas, 1994; Schweisguth and Posakony, 1992). Functioning in this role, which dates at a minimum to the last common ancestor of demosponges and eumetazoa (Richards and Degnan, 2012), Su(H) participates in a huge variety of conditional cell fate specification events in virtually all metazoans.

It came as a surprise, then, to find that Su(H) has been coopted in *Drosophila* for a very different role: acting as an essential regulator of the differentiation of the socket cell, a nonneuronal component of external sensory organs in the fly (Figure 1A; Barolo et al., 2000). Regulation of Notch pathway target genes by Su(H) requires only a low basal level of the protein, which is present broadly or ubiquitously. But in *Drosophila*, Su(H) is in addition very highly expressed specifically in socket cells, beginning soon after the birth of the cell via the division of the pIIa secondary precursor and continuing stably thereafter (Figures 1A, 1D, and 1D′; Barolo et al., 2000; Miller et al., 2009). This high level of transcript and protein accumulation from *Su(H)* is driven by a dedicated transcriptional control module, the autoregulatory socket enhancer (ASE). The ASE lies downstream of the gene, includes eight high-affinity Su(H) binding sites, and mediates a direct positive autoregulation activity specifically in socket cells (Figures 1B, 1C, and 1E–1F′).

Although the fate of the socket cell is specified by Notch signaling, the ASE plays no role in this—indeed, the enhancer's activity does not commence until after the cell's fate has already been determined. Rather, mechanosensory organs in a fly lacking the ASE display severely impaired mechanotransduction, evidently due to defects in socket cell differentiation (Barolo et al., 2000). In addition, the socket cell autoregulatory activity of Su(H), acting in concert with the socket cell-specific transcription factor Sox15, is also required to prevent deployment of an alternative differentiative program, that of the shaft cell, the socket cell's sister (Figure 1A; Miller et al., 2009). This is accomplished by repressing expression of *shaven* (*sv*), which encodes a high-level regulator of shaft cell differentiation (Kavaler et al., 1999).

A previous study from our laboratory (Barolo et al., 2000) revealed that the ASE is initially activated by the Notch signaling event that specifies the socket cell fate. Here, a low level of Notch-stimulated Su(H) functions cooperatively with certain "local activators" that are expressed in both the socket and shaft cells (Figures 1A and 1B). By contrast, the long-term maintenance of high-level *Su(H)* autoregulation was found to be independent of Notch.

Despite the prevalence of positive autoregulation by transcription factor-encoding genes as a developmental control strategy,
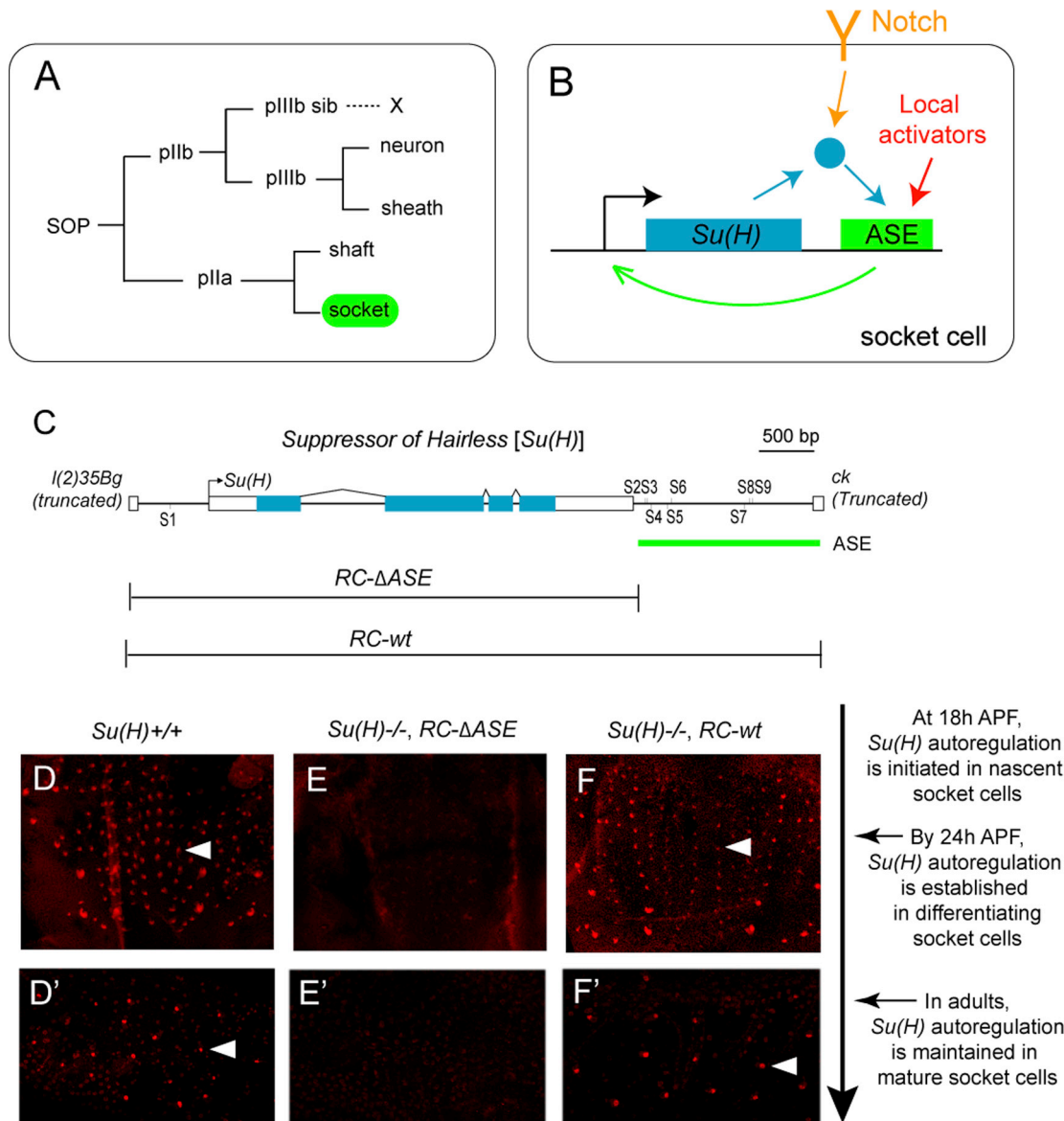
Figure 1. The ASE Controls Transcriptional Autoactivation of *Su(H)* in the Socket Cell

(A) Lineage of *Drosophila* adult external mechanosensory organs. The socket cell is highlighted in green. SOP, sensory organ precursor cell.

(B) *Su(H)* autoactivates its expression specifically in the socket cell via a dedicated *cis*-regulatory module, the autoregulatory socket enhancer (ASE) (Barolo et al., 2000). The socket cell-specific activation of the ASE is dependent on synergies between Notch signaling, via Su(H), and inputs from other activators in the sensory organ lineage (Barolo et al., 2000).

(C) Diagram of the *Su(H)* gene. The ASE is included within a 1.9 kb genomic segment located downstream of *Su(H)* and contains eight high-affinity Su(H) binding sites (S2–S9) (Barolo et al., 2000). The *RC-wt* genomic DNA fragment fully rescues all known functions of *Su(H)* when placed in a *Su(H)* null mutant background; *RC-ΔASE* lacks the ASE and hence the autoregulatory activity of the gene, but it rescues all ASE functions, including the broad basal level of Su(H) expression (see D–F and D′–F′) (Barolo et al., 2000).

(D–F′) Anti-Su(H) antibody (red) marks the high level of the protein in socket cells in the pupal notum at 24 hr after puparium formation (APF) (D–F) and in the abdominal epithelium of adult flies (D′–F′). Note the lack of strong staining in the $Su(H)^{-/-}$; *RC-ΔASE* genotype (E and E′). Individual socket cells are indicated by arrowheads. $Su(H)^{-/-}$ refers to the null genotype $Su(H)^{AR9}/Su(H)^{SF8}$ (Barolo et al., 2000; Schweisguth and Posakony, 1992). The relationship between the imaging time points and the development of microchaete socket cells is described to the right of these panels.

the specific mechanisms by which the autoregulatory state is initiated, established, and maintained have not been studied in detail. We have chosen the *Su(H)* ASE as a model for investigating this question. Dissecting a direct transcriptional autoregulatory activity necessitates separately analyzing the associated enhancer's ability to respond to the normal wild-type context, with its normal level of the autoregulatory factor (e.g., by examining the expression of reporter transgene variants in a wild-type background) and its ability to establish the autoregulatory state (e.g., by examining levels of the autoregulatory factor generated
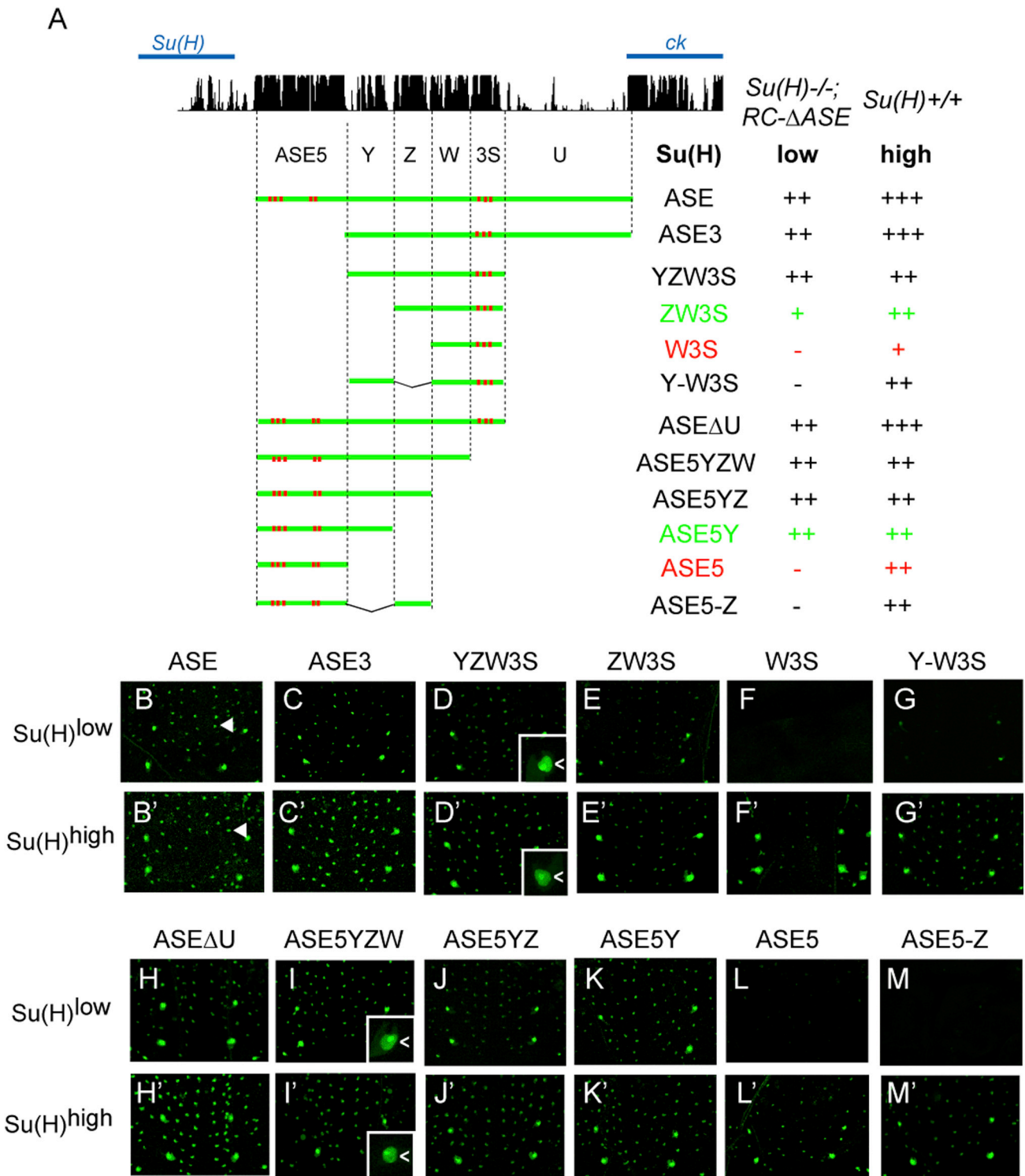
Figure 2. Identification of Functional Sequence Elements of the ASE in the Nascent Socket Cell

(A) The pattern of conservation of ASE sequences in *Drosophila* species, as displayed by the UCSC genome browser (http://genome.ucsc.edu/), is shown at the top. Diagrams of ASE fragments (green lines) tested in GFP reporter transgene constructs are shown below. Previously identified Su(H) binding sites are marked in red. Observed levels of GFP expression in nascent socket cells are summarized at right. Reporter gene activities were assayed in two genetic backgrounds: wild-type ($Su(H)^{+/+}$ or Su(H)^{high}) and $Su(H)^{-/-}$; RC-ΔASE (only the basal level of Su(H), or Su(H)^{low}). GFP levels were scored using the following semiquantitative system: strong, +++; moderate, ++; weak, +; weak stochastic, −/+; and negative, −. Two comparisons (ZW3S/W3S and ASE5Y/ASE5) are highlighted in green/red type.

(legend continued on next page)

by genomic rescue construct variants in a genetic background lacking the function of the autoregulatory gene). We have studied these two capabilities in detail in exploring the ASE's mechanism of operation.

Counter to the expectation that the ASE functions as a single modular enhancer unit, our investigation reveals that it is instead composed of several overlapping structural and functional elements that we refer to as enhancer submodules, each of which can independently become active in the differentiating socket cell. Moreover, because each of the ASE's submodules contains one or a few Su(H) binding sites, together they form several interlinked positive feedback loops with the *Su(H)* gene. Interestingly, not all of the ASE's autoregulatory submodules respond to Su(H) equally: although some are activated by a low level of Su(H), others require much higher levels. As a result, the different submodules are deployed in succession: first to initiate a low-level autoregulatory activity, then to establish the autoregulatory state by exceeding a threshold level of Su(H), and finally to "lock down" a permanent high-level maintenance function. We propose a coherent model that explains how the ASE rapidly translates an initiating Notch pathway input signal into a highly elevated and irreversible level of Su(H) expression, specifically in the developing socket cell. We suggest that enhancer subfunctionalization via enhancer submodules may be a generalizable mechanism for integrating inputs from a suite of dynamically expressed *trans*-regulators into a stable gene expression state.

RESULTS

Molecular Dissection of the ASE

We began the detailed analysis of the ASE's function by asking if its initial activity in the nascent socket cell is dependent on the ASE-*Su(H)* autoregulatory feedback loop. To address this question, we used a transgenic reporter gene assay to examine the ASE's activity in a *Su(H)* null mutant background that also carries a genomic DNA rescue construct (*RC-ΔASE*) capable of rescuing only the low basal level of *Su(H)* expression (see Figures 1C–1F'; Barolo et al., 2000). As shown in Figures 2A and 2B, an *ASE-GFP* reporter is active at substantial levels specifically in the nascent socket cell, despite the low level of Su(H) in these flies (*Su(H)$^{-/-}$; RC-ΔASE*, or Su(H)^{low}; see Figure 1E). This result indicates that the initial phase of the ASE's activity is independent of its autoregulatory function.

Next, to determine which part(s) of the ASE is required for its early activity, we tested the *cis*-regulatory activities of a series of deletion constructs in the Su(H)^{low} mutant background (Figure 2A). Interestingly, we find that the ASE contains two nonoverlapping fragments—ZW3S and ASE5Y (Figure 2A)—that can independently become active in the nascent socket cell (Figures 2A, 2E, and 2K). Consistent with an important functional role for these fragments, the sequences of both ZW3S and ASE5Y are highly conserved among *Drosophila* species (Figure 2A).

In an earlier study, a small fragment called ASE5, which is part of ASE5Y (Figure 2A), was shown to be strongly active in the

socket cell in a wild-type background (*Su(H)$^{+/+}$*, or Su(H)^{high}; see Figures 1D and 1D') (Barolo et al., 2000). However, ASE5 is completely silent in the Su(H)^{low} background (Figure 2L), which suggests that its activity must rely on a certain threshold level of Su(H). On the other hand, that ASE5Y, but not ASE5, is active in the Su(H)^{low} background suggests that fragment Y mediates important activator input(s) (compare Figures 2K and 2L). However, unlike ASE5, Y alone shows no detectable activity even in the wild-type Su(H)^{high} background (Figures 3A and 3B), suggesting that Y does not respond to Su(H). Indeed, Y contains no sequence motif that resembles a Su(H) binding site, whereas ASE5 contains five (S2–S6; see Figures 1C and 2A) (Barolo et al., 2000).

Remarkably, ZW3S shares a similar bipartite organization with ASE5Y. It includes a small fragment, called W3S (Figure 2A), which by itself is active in the wild-type Su(H)^{high} background but is silent in the mutant Su(H)^{low} background (Figures 2F and 2F'). The remaining portion of ZW3S, fragment Z (Figure 2A), though required for generating ZW3S's activity in the Su(H)^{low} background (compare Figures 2E and 2F), is silent in the socket cell even in the wild-type Su(H)^{high} background (Figures 3A and 3C). Thus, W3S acts like ASE5 in responding to Su(H) in a dose-dependent manner, and Z functions like Y in mediating weak Su(H)-independent activator input(s). As in the case of ASE5 and Y, this functional difference between W3S and Z is also likely because W3S contains a cluster of three Su(H) binding sites (S7–S9; see Figures 1C and 2A), whereas Z contains none.

Despite the similarities between ASE5Y and ZW3S in their structure and function, we found that their components are not interchangeable, inasmuch as two synthetic constructs, one consisting of artificially linked ASE5 and Z (ASE5-Z; Figure 2A) and the other of Y and W3S (Y-W3S; Figure 2A), show little activity in the socket cell in the Su(H)^{low} background (Figures 2G and 2M). Thus, ASE5Y and ZW3S act as distinct enhancer modules in the socket cell, with their *cis*-regulatory activities being respectively dependent on specific synergies between ASE5 and Y, and between Z and W3S.

These results suggest that four fragments—ASE5, ASE5Y, W3S, and ZW3S—represent distinct enhancer submodules, each making a unique contribution to the temporal and quantitative activity of the ASE in the socket cell.

Fragment YZW Responds to Weak Activator Inputs in the Shaft and Socket Cells

Whereas the ASE fragments described above all show socket cell-specific *cis*-regulatory activities, another fragment called YZW—which includes all sequences between the two clusters of Su(H) binding sites (S2-S6 and S7-S9; see Figures 1C and 2A)—is active in both the socket cell and the shaft cell in the pupal-stage notum (Figures 3H and 3L–3O; see also Figure 1A; Figure S1 available online). We divided YZW into three smaller pieces (Y, Z, and W) and found that none of them showed any detectable enhancer activity (Figures 3A–3D); the same result

(B–M) GFP expression in the pupal notum at 24 hr APF; Su(H)^{low} background, lacking the autoregulatory activity of *Su(H)*. (B'–M') GFP expression in the pupal notum at 24 hr APF; wild-type (Su(H)^{high}) background.
Arrowheads in (B) and (B') mark the positions of single mechanosensory organs. Insets in (D), (D'), (I), and (I') show socket cell (<) specificity of GFP expression.
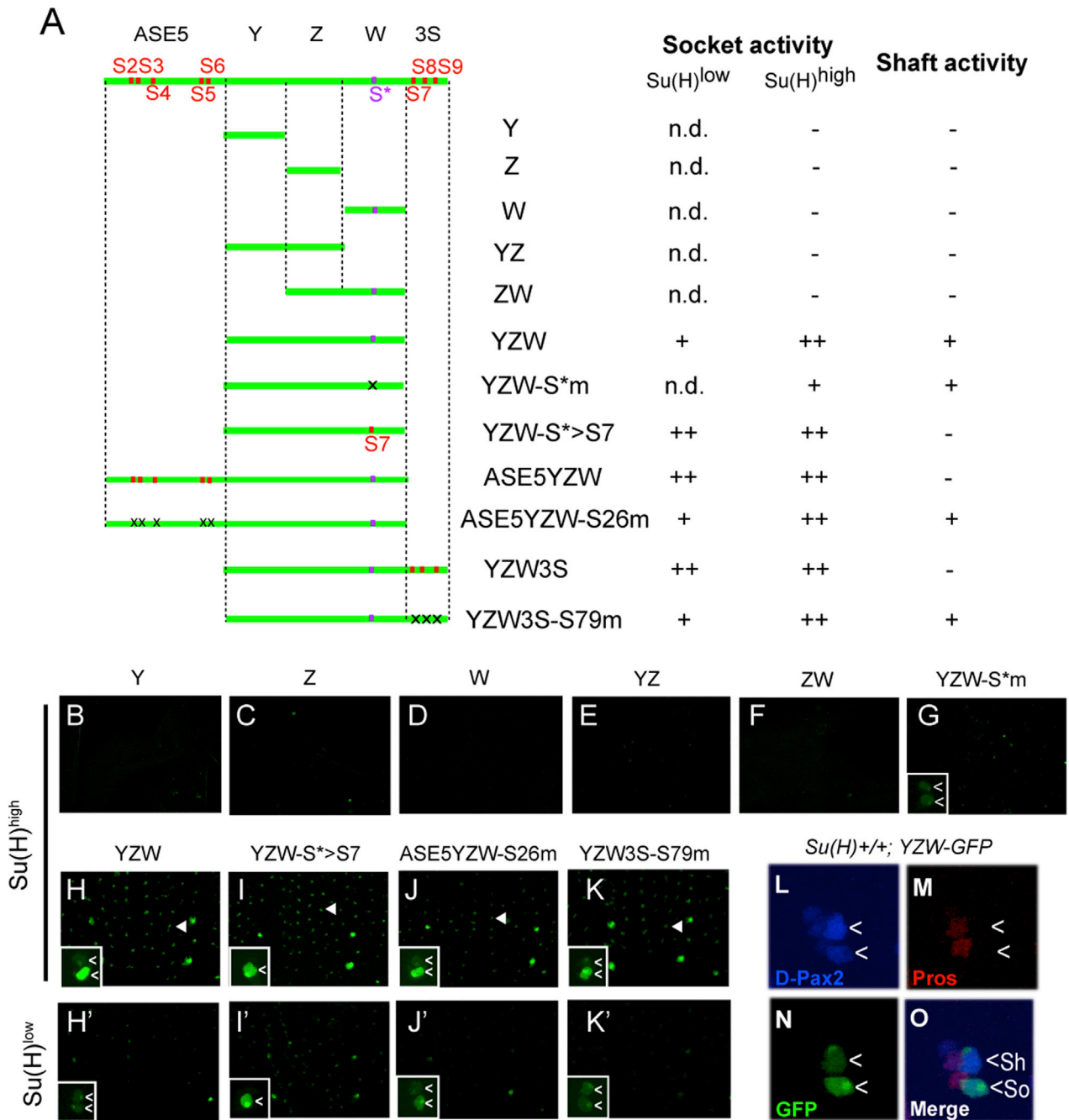
Figure 3. The ASE Is Activated by the Synergistic Function of a Low Level of Su(H) and Weak Local Activators

(A) Diagrams of ASE fragments (green lines) tested in GFP reporter transgene constructs in the pupal notum at 24 hr APF. Previously identified Su(H) binding sites (S2–S9) are marked in red; a Su(H) binding site, S*, identified here is marked in purple. Mutated Su(H) binding sites are indicated by "x." Observed levels of GFP expression are summarized at right, using the same semiquantitative scoring system as in Figure 2. "n.d." means not determined.

(B–K) GFP expression in the pupal notum at 24 hr APF in the wild-type (Su(H)^high) background. Arrowheads in (H)–(K) mark the positions of single mechanosensory organs. (H′–K′) GFP expression in the pupal notum at 24 hr APF in the mutant (Su(H)^low) background (*Su(H)^{−/−}; RC-ΔASE*) lacking the autoregulatory activity of *Su(H)*. Insets in (G)–(K) and (H′)–(K′) show higher-magnification views of GFP expression at single mechanosensory organ positions. Cells displaying GFP signal are marked (<).

(L–O) The YZW fragment of the ASE drives weak expression in both the shaft (Sh) and socket (So) cells (denoted by <). Shown is a single developing mechanosensory organ in the pupal notum at 20 hr APF in the wild-type background. (L) The cells of the mechanosensory organ lineage (see Figure 1A) are marked by anti-D-Pax2 antibody (blue); the strongest signal is in the shaft cell (Kavaler et al., 1999). (M) The cells of the pIIb branch of the lineage are marked by anti-Prospero (Pros) antibody (red). (N) Anti-GFP antibody (green) marks the activity of the *YZW-GFP* transgene. (O) Merged three-channel image. The socket and shaft cells are distinguished by their enlarged nuclei (due to endoreplication) and lack of anti-Prospero reactivity.

See also Figures S1–S3.

was obtained with the YZ and ZW combinations (Figures 3A, 3E, and 3F). Thus, the dual shaft/socket activity of YZW derives from the synergistic action of weak activator inputs that are distributed among the three separate segments (see also Figure S2).

Curiously, although no Su(H) binding site was previously identified in YZW, this fragment's socket cell activity is significantly greater in the Su(H)^{high} background than in the Su(H)^{low} background, whereas its shaft cell activity does not exhibit such a difference (Figures 3H and 3H'). Two lines of evidence indicate that the Su(H) dose dependence of YZW's socket cell activity is mediated by a Su(H) binding motif (CCTGAGAA) we found in the W fragment (Figure 3A). First, this motif, which we call S*, binds a purified 6XHis-Su(H) fusion protein in vitro in a sequence-specific manner (see Figure S3F). Second, when S* is mutated, YZW's socket cell activity in the wild-type (Su(H)^{high}) background is severely weakened, so that it now functions at similarly low levels in both the shaft cell and the socket cell (compare Figures 3G and 3H; see also Figures S3A–S3E). This effect is essentially the same as reducing the Su(H) level in the socket cell, that is, by placing YZW in the Su(H)^{low} background (Figure 3H'). We conclude that S* responds directly to a high level of Su(H) to promote YZW's activity in the socket cell.

In an earlier study, it was shown that Su(H) binding sites S2–S9 in the ASE (see Figure 1C) mediate a transcriptional repression function of Su(H) in the shaft cell (where Notch is "off") (Barolo et al., 2000), but the activity of YZW in the shaft cell indicates that S* does not function in this way. In support of this interpretation, we find that simply replacing S* with S7, the nearest Su(H) site that conforms to the canonical motif definition YGTGDGAA, results in nearly complete silencing of YZW in the shaft cell (compare Figures 3H and 3H' and Figures 3I and 3I'). Furthermore, it is notable that the S*-to-S7 mutation also resulted in an increased activity of YZW in the socket cell under Su(H)^{low} conditions (compare Figures 3H' and 3I'). Together, these observations indicate that, in comparison with S7, S* is a functionally weaker Su(H) binding site: it does not mediate significant repression in the shaft cell, and does not mediate a strong activation function in the socket cell. The weakness of S* is likely due to the fact that its sequence (CCTGAGAA) differs by one base (underlined) from the high-affinity Su(H) binding motif definition (YGTGDGAA) (Bailey and Posakony, 1995; Barolo et al., 2000; Nellesen et al., 1999; Tun et al., 1994). We note that the functional importance of the S* site is supported by its conservation in all of the original 12 Drosophila species with sequenced genomes and by the observed effect of mutating it in the context of the full-length Su(H) rescue construct (see Figures S3G and S3H).

In summary, then, these experiments indicate that YZW includes binding sites for a pIIa lineage-specific factor or factors that generate comparably weak cis-regulatory activity in the shaft and socket cells, along with a weakened Su(H) binding site S*, which can promote the socket cell activity of YZW, but only when Su(H) is present at high levels.

The Basal Level of Su(H) Synergizes with Weak Local Activators to Trigger Strong Activation of the ASE in the Nascent Socket Cell

As shown above, fragment ASE5, which contains Su(H) binding sites S2–S6, is active in the wild-type (Su(H)^{high}) background but is completely silent in the Su(H)^{low} background. Although the latter result may suggest that S2–S6 do not respond to basal levels of Su(H), we observed that ASE5YZW—which includes the sequences of both ASE5 and YZW—is substantially more active than YZW in the socket cell when both are assayed in the Su(H)^{low} background (compare Figures 2I and 3H'). Importantly, this difference is abolished by mutation of sites S2–S6 (Figures 3H' and 3J'), suggesting that the Su(H) input via S2–S6 in ASE5 can synergize with inputs on YZW to promote the latter's socket cell activity, even when Su(H) is present at low levels. In a similar vein, we find that Su(H) binding sites S7–S9 can likewise promote the socket cell activity of YZW in the Su(H)^{low} background (compare YZW3S [Figure 2D] and YZW3S-S79m [Figure 3K']).
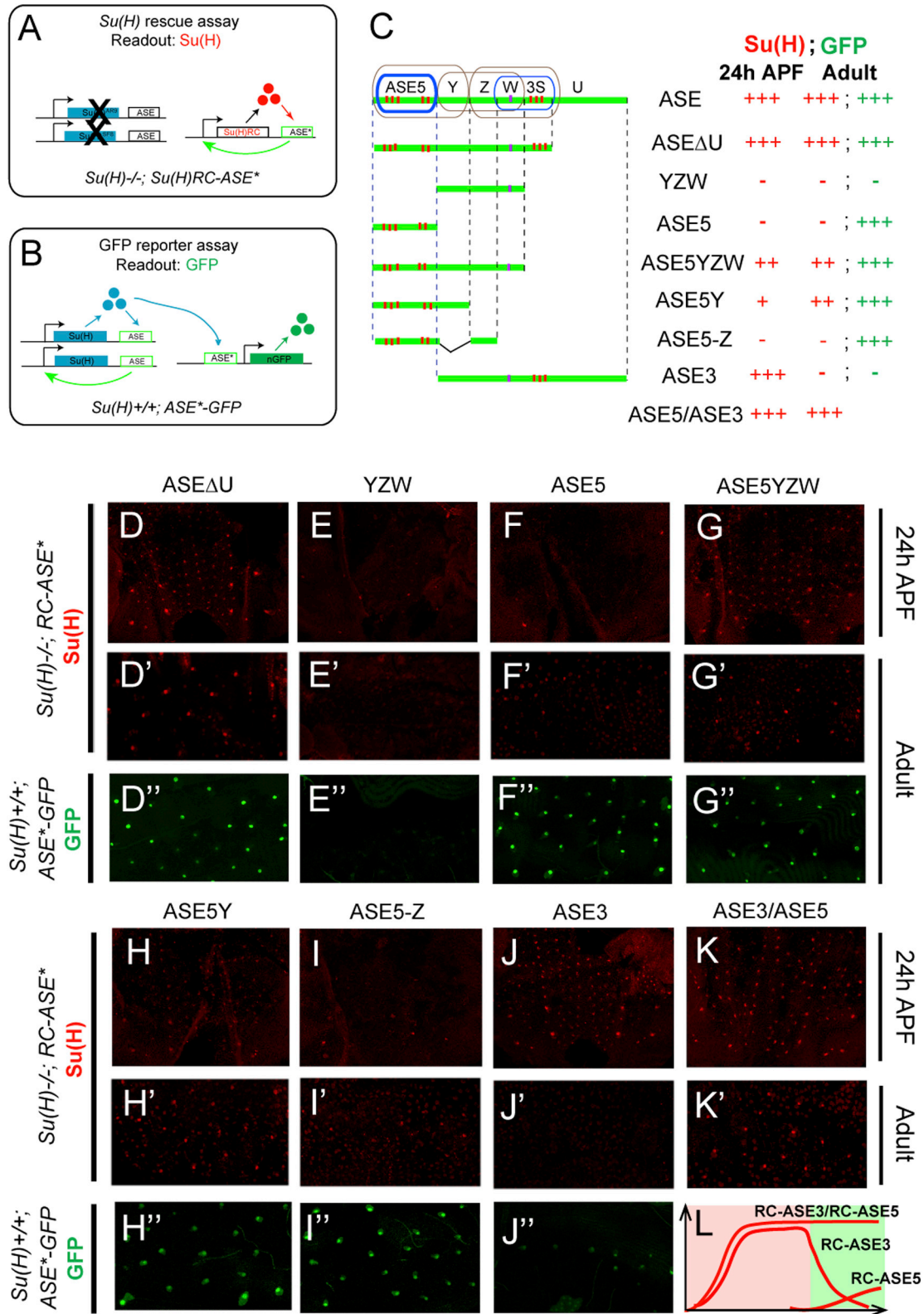
Together, these experiments reveal the cis-regulatory logic underlying the initiation of the ASE's activity in the socket cell: it is combinatorially activated by the basal level of Su(H), which acts upon two separate clusters of high-affinity Su(H) binding sites (S2–S6 and S7–S9), and by certain weak "local activators," which act upon the YZW fragment to generate—independent of Su(H)—a baseline level of activity in both the shaft cell and the socket cell. The basal level of Su(H) acts cooperatively with the "local activators" in the socket cell, while at the same time repressing their function in the shaft cell, resulting in a socket cell-specific initial activity of ASE.

Synergistic Inputs on the ASE Are Required to Initiate Su(H) Autoregulation

The experiments described thus far delineate three segments of the ASE (ASE5Y, YZW, and ZW3S) that display cis-regulatory activities in the nascent socket cell that do not require an above-basal level of Su(H). Because the role of the ASE in development is to form a strong positive feedback loop with Su(H), we reasoned that these fragments may be involved in initiating this loop.

To determine more specifically how the ASE-Su(H) feedback loop is established, we placed several ASE truncations downstream of the minimum Su(H) rescue construct (RC-ΔASE) and asked if they are able to drive expression of the transgene in a Su(H) null background (Su(H)$^{-/-}$) (Figure 4A). In this Su(H) rescue assay, we first focused on YZW and ASE5, which respond primarily to the socket/shaft activators and Su(H), respectively. As summarized in Figure 4C, neither YZW nor ASE5 is able to drive significant Su(H) transgene expression in the nascent socket cell (Figures 4E and 4F). By contrast, ASE5YZW, which includes the sequences of both ASE5 and YZW, supports strong Su(H) transgene activity in the nascent socket cell (Figure 4G; see also Figures S4B and S4E), suggesting that synergistic interaction between ASE5 and YZW is required to initiate high levels of Su(H) expression in this cell.

Next, to verify the specificity of interaction between certain cis-elements of the ASE in establishing Su(H) autoregulation, we also compared the activities of the fragment ASE5Y and the synthetic construct ASE5-Z in the Su(H) rescue assay (Figures 4H and 4I). We found that ASE5Y can drive weak, but significant, Su(H) transgene expression in the nascent socket cell (Figure 4H; see also Figures S4C and S4F), whereas the synthetic construct ASE5-Z almost completely failed to generate significant above-basal levels of Su(H) (Figure 4I). Thus, consistent with the earlier experiments using a GFP reporter assay (see

Figure 4. The ASE's Submodules Dynamically Control *Su(H)* Autoregulation

(A) The *Su(H)* transgene rescue assay. Left: The endogenous *Su(H)* autoregulatory loop is disrupted by *Su(H)* null mutations (X's). Right: The *Su(H)* gene (Su(H)RC) and ASE* (wild-type ASE or fragment thereof) carried in the rescue transgene construct form a positive feedback loop. Anti-Su(H) antibody staining is used as the readout, indicating whether ASE* is sufficient to establish *Su(H)* autoregulation in the socket cell.

(legend continued on next page)

Figures 2K and 2M), ASE5 selectively synergizes with Y, but not Z, to contribute to the initiation of *Su(H)* autoregulation.

Only ASE5 Is Responsible for Maintaining *Su(H)* Autoregulation

Although the socket/shaft factors acting upon YZW are required for the ASE's initial activity in the nascent socket cell, we find that this fragment displays no detectable activity in the adult socket cell (Figures 4E′ and 4E″), indicating that some or all of the socket/shaft activators are only transiently expressed in the socket cell and may thus be required only for the initiation, but not for the maintenance, of the ASE's activity in this cell.

As mentioned earlier, the ASE contains two Su(H) response elements, ASE5 and W3S (Figure 2A), both of which require above-threshold levels of Su(H) for activation. Because both ASE5 and W3S can drive significant reporter gene activity in the adult socket cell (Figures 4F″, S7C, and S7F), we reasoned that they may be required to maintain the autoregulation of *Su(H)* in this cell, in which Su(H) is expressed at high levels. Unexpectedly, we find that deleting ASE5 from the ASE (ASE3; Figure 4C) results in almost complete loss of the above-basal level of Su(H) expression in the adult socket cell (Figures 4J′ and 4J″). By contrast, two rescue constructs, *RC-ASE5Y* and *RC-ASE5-Z*, can both drive significant *Su(H)* transgene expression in adult socket cells, even though they lack the W3S segment (Figures 4H′, 4H″, 4I′, and 4I″). Thus, even though both ASE5 and W3S can function as Su(H) response elements, only ASE5 is strictly required for the autoregulated expression of *Su(H)* in adults.

Consistent with an essential role for ASE5 in mediating the ASE's function in adult socket cells, we find that, in the GFP reporter gene assay, the *cis*-regulatory activity of ASE5 is comparable to that of the full ASE in adults, whereas ASE3, which includes all of the ASE except ASE5, is almost silent in adults (Figures 4D″, 4F″, and 4J″; see Figures S7B–S7D). These observations suggest that the ASE's activity in adults can be attributed primarily to one Su(H) response element, ASE5. In addition, they suggest that the *cis*-regulatory activity of the other Su(H) response element, W3S, is repressed in adults in the context of the full ASE, presumably because of negative inputs mediated by nearby sequences (see Figures S7D–S7F).

Taken together, these experiments indicate that ASE5 is both necessary and sufficient to account for the ASE's activity in the adult socket cell. We conclude that the ASE's function in adults—long-term maintenance of *Su(H)* autoregulation—is carried out by ASE5.

The ASE's Submodules Are Functionally Interlinked

One notable finding from the above experiments is that two nonoverlapping components of the ASE, ASE3 and ASE5, exhibit temporally distinct *cis*-regulatory activities during development. On the one hand, whereas ASE3 can stimulate strong *Su(H)* autoregulation in the socket cell in the early pupal stage (see Figure 4J), its activity decreases over time (see Figures 4J′ and 4J″). On the other hand, although ASE5 cannot initiate *Su(H)* autoregulation in the pupal stage (see Figure 4F), it is required for maintaining the late phase of the ASE's activity in adults. Thus, these two separate parts of the ASE appear to be involved in mediating *Su(H)* autoregulation at different stages of development.

Because ASE3 can transiently drive strong Su(H) expression in the socket cell in early pupae, we hypothesized that this early activity of ASE3 may function to provide the necessary threshold level of Su(H) required to activate ASE5. In support of this hypothesis, although *ASE5-GFP* is not expressed at any stage in a Su(H)^{low} background ($Su(H)^{-/-}$; RC-ΔASE), we found that replacing *RC-ΔASE* with *RC-ASE3* in the *Su(H)* null background resulted in significant *ASE5-GFP* expression in the socket cells of the pupal notum, starting from as early as 28 hr APF (Figures 5A and 5C).

To explore this further, we placed one copy each of *RC-ASE5* and *RC-ASE3* in the *Su(H)* null background and examined the resulting level of Su(H) in the socket cell. We found that flies of this genotype ($Su(H)^{-/-}$; RC-ASE3/RC-ASE5) strongly express Su(H) in the socket cell at both pupal and adult stages (Figures 4K–4K′). Because neither *RC-ASE5* alone nor *RC-ASE3* alone is able to establish robust high levels of Su(H) expression in adults (Figures 4F′ and 4J′), and given that ASE3 exhibits little GFP reporter gene activity in adults (Figure 4J″), the appearance of high levels of Su(H) in adult flies of the $Su(H)^{-/-}$; RC-ASE3/RC-ASE5 genotype demonstrates an ability of these two nonoverlapping elements to communicate and cooperate even when they are separate rather than adjacent (Figure 4L). This finding provides strong support to the conclusion that autoregulatory submodules of the ASE are functionally interlinked.

Control of the Timing of the Initiation-Maintenance Transition in *Su(H)* Autoregulation

The above experiments demonstrate an intriguing feature of the ASE's functional organization: initiation of its activity requires a significantly larger part of the enhancer than its maintenance. Specifically, initiation in the nascent socket cell is dependent on several seemingly redundant enhancer submodules (ASE5Y, YZW, and ZW3S), but maintenance in the adult socket cell is dependent only on ASE5, which is but a small part of the ASE.

(B) GFP reporter transgene assay in the wild-type background. Once the endogenous ASE-*Su(H)* feedback loop is established (left), its output (Su(H)) acts on the ASE fragment (ASE*) carried in the reporter transgene construct to drive GFP expression (right). GFP fluorescence in adult flies is used as the readout, indicating whether ASE* is able to respond to the high maintenance levels of Su(H).

(C) Diagrams of ASE fragments (green lines) tested in both the *Su(H)* transgene rescue and GFP reporter transgene assays. Submodules of the ASE are encircled: brown indicates a submodule active in the Su(H)^{low} background in pupal stages; blue indicates a submodule active only in the Su(H)^{high} background in pupal stages. Observed levels of Su(H) and GFP expression are summarized at right, using the same semiquantitative scoring system as in Figure 2.

(D–K) *Su(H)* rescue assay: anti-Su(H) antibody staining in the pupal notum at 24 hr APF. (D′–K′) *Su(H)* rescue assay: anti-Su(H) antibody staining in the adult abdominal epithelium. (D″–J″) GFP reporter assay: GFP expression in socket cells in the adult abdominal epithelium.

(L) Cartoon illustration of Su(H) expression in the *Su(H)* rescue assays using *RC-ASE3*, *RC-ASE5*, or *RC-ASE3/RC-ASE5*. Pink panel indicates pupal stage; green panel indicates adult stage; and red lines indicate levels of Su(H) expression (relative levels are arbitrary).

See also Figure S4.
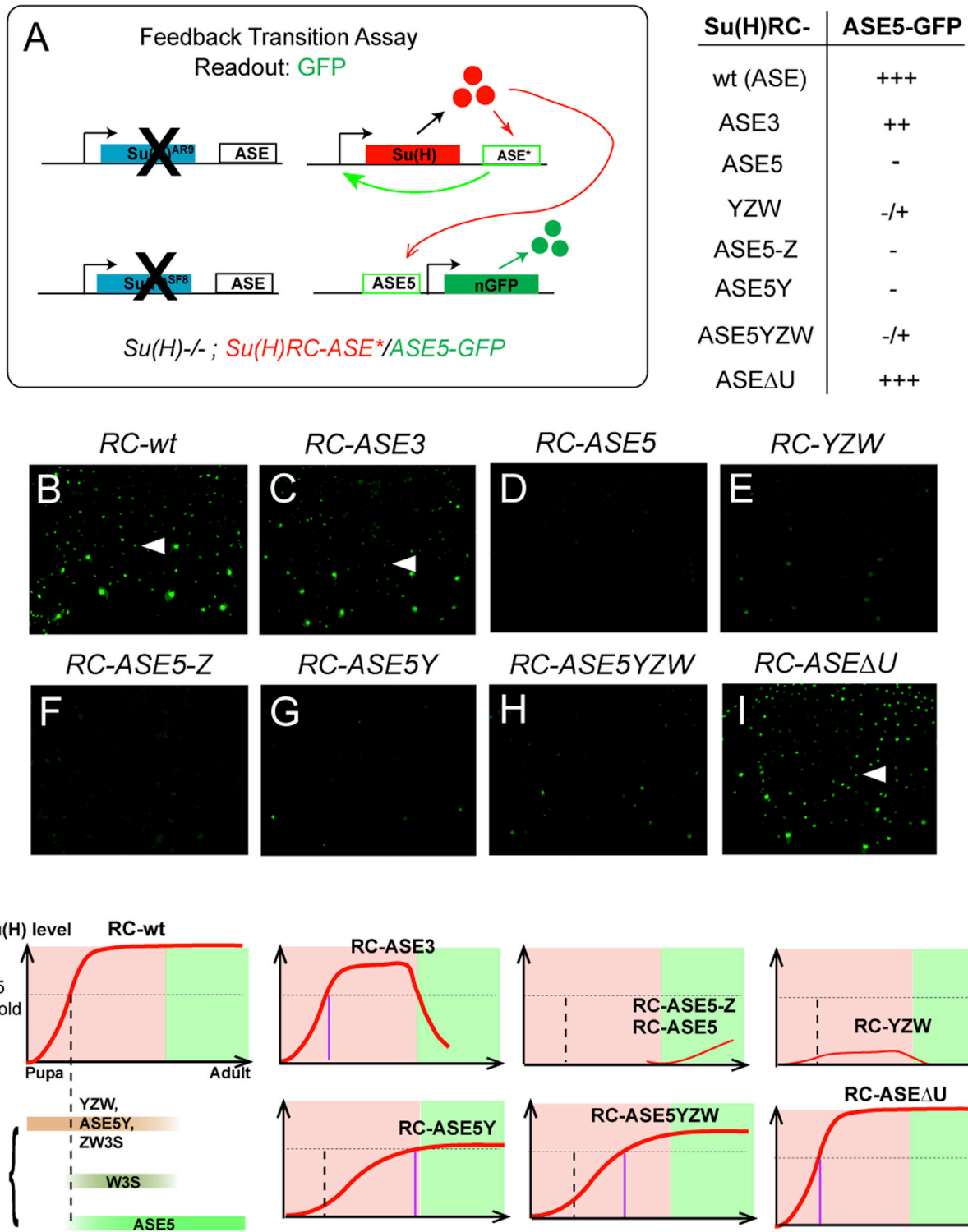
Figure 5. The Transition from Initiation to Maintenance of *Su(H)* Autoregulation Depends on Interlinked Functions of the ASE's Submodules

(A) Diagram of the feedback transition assay. One copy each of a *Su(H)* rescue construct and the *ASE5-GFP* reporter construct, both on the third chromosome, are placed into the *Su(H)* null background. Observed levels of GFP expression are summarized at right, using the same semiquantitative scoring system as in Figure 2.

(B–I) Activity of the *ASE5-GFP* reporter in the pupal notum at 28 hr APF in the *Su(H)*$^{-/-}$; *RC-ASE** background. Arrowheads in (B), (C), and (I) indicate single microchaete socket cells that express high levels of GFP.

(legend continued on next page)

Because a certain high level of Su(H) is required to activate ASE5 (Figures 2L–2L′), we reasoned that the involvement of multiple initiation submodules may be important to ensure that Su(H) reaches the required threshold level for this activation. To test this idea more systematically, we examined the expression of the *ASE5-GFP* reporter gene at the pupal stage in various *Su(H)* rescue genotypes (Figure 5A). We found a strong correlation between the activity of *ASE5-GFP* and the extent of the enhancer sequences included in the *Su(H)* rescue construct. In particular, although five rescue constructs can drive significant Su(H) expression in the nascent socket cell, only three—*RC-wt*, *RC-ASE3*, and *RC-ASEΔU*—can consistently stimulate strong *ASE5-GFP* activity in the pupal notum at 28 hr APF (Figures 5B–5I; see also Figures S5 and S6). By contrast, even though both *RC-ASE5Y* and *RC-ASE5YZW* are also able to generate significant Su(H) expression in the nascent socket cell (see Figures 4G and 4H; see also Figure S4), the levels of rescued Su(H) in these genotypes do not appear to be high enough to activate *ASE5-GFP* robustly in socket cells at this stage (Figures 5G and 5H).

These experiments suggest that the minimum requirement for stable activation of the *ASE5-GFP* reporter in early pupae is for the rescue construct to include the sequences of the two initiation submodules YZW and ZW3S (shared by ASEΔU and ASE3; see Figure 4C), even though neither of them is essential for the late activity of ASE5 or for the maintenance of Su(H) autoregulation in adults. Therefore, although many of the functionally important components of the ASE are only transiently active in development, they contribute quantitatively to the initial increase of Su(H) expression in the nascent socket cell and thus are involved in controlling the timing of the transition into the maintenance phase of *Su(H)* autoregulation (Figure 5J).

Combinatorial Activation of ASE5 in the Pupal Stage Is Required to Establish *Su(H)* Autoregulation in Adults

In a previous study (Liu and Posakony, 2012), we analyzed the functional architecture of ASE5 and found that its activity in the socket cell relies not only on the five Su(H) binding sites (S2–S6; Figure 6A) but also on two other types of sequence motif. The first is a single 11 bp sequence element (AACGCGAAGCT, or A motif), and the other comprises four high-affinity binding sites for the POU-homeodomain factor Ventral veins lacking (Vvl) (Figure 6A). The A motif and the Vvl sites are both required for ASE5's activation in the pupal stage, but they become somewhat redundant in adults. Thus, mutation of either the A motif or the Vvl binding sites each results in severe reduction of ASE5's activity in the pupal stage, while having relatively little effect on its function in adults (Liu and Posakony, 2012).

To investigate the possible roles of the A motif and the Vvl sites in *Su(H)* autoregulation, we mutated them separately in the context of the wild-type *Su(H)* rescue construct (*RC-wt*; Figure 6A). We found that these two types of mutation had

little effect on the ability of *RC-wt* to establish high levels of Su(H) expression in the pupal stage, but in both cases, the early high level of Su(H) is lost in the adult socket cell (Figures 6B–6D′). This is similar to the effect of mutating all five Su(H) binding sites in ASE5 (S2–26) in the context of *RC-wt* (Figures 6E and 6E′).

Based on the "phase transition" model described above, we suggest that these results can be explained by the failure of ASE5 to be activated in a timely manner in the differentiating socket cell. That is, the apparently normal rescue of Su(H) expression observed in the pupal stage in these genotypes is driven by an early phase of the ASE's activity, which is mediated by the sequences outside of ASE5 (i.e., ASE3). However, in the absence of input via the A motif, the Vvl sites, or the Su(H) binding sites, ASE5 remains silent at the time ASE3's activity declines and disappears, so that the transient expression of high levels of Su(H) cannot be maintained in adults (Figure 6F).

DISCUSSION

A Dynamic Model of the Control of *Su(H)* Autoregulation

In this study, we have systematically dissected the functional organization of the autoregulatory socket enhancer (ASE) of the *Drosophila Su(H)* gene, which controls the long-term transcriptional autoactivation of *Su(H)* specifically in the socket cell of external sensory organs (Barolo et al., 2000). Based on these experiments, we propose a dynamic model to explain how *Su(H)* autoregulation is controlled (Figure 7).

We suggest that, within a short time window (0–2 hr) after the division of the pIIa secondary precursor cell (see Figure 1A), the ASE receives certain "local activator" inputs in both postmitotic daughter cells via the YZW fragment; at the same time, the ASE is silenced by the repressive activity of basal levels of Su(H), via the two flanking clusters of high-affinity Su(H) binding sites, S2–S6 and S7–S9 (Figure 7A).

Next, the incoming Notch signal that specifies the socket cell fate converts Su(H) into a transcriptional activator in this cell (Barolo et al., 2000); Su(H) then synergizes with the early inputs on YZW to activate two enhancer submodules, ASE5Y and ZW3S, to trigger a rapid rise in *Su(H)* transcription. Simultaneously, YZW may contribute independently to the activity of *Su(H)*. The activation of these three submodules marks the initiation of the ASE-*Su(H)* autoregulatory loop (Figure 7B).

Later, about 4 hr after the socket cell is born, the accumulated level of Su(H) rises above a certain threshold and feeds back on the ASE to activate two Su(H) response elements, ASE5 and W3S, the activities of which are strictly Su(H) concentration dependent. Moreover, at least for ASE5, Su(H) must synergize with two other activator inputs that are mediated by the A-motif and several high-affinity Vvl binding motifs (Liu and Posakony, 2012). The activation of ASE5 and W3S marks the time when the ASE-*Su(H)* autoregulatory loop is fully established (Figure 7C).

(J) Cartoon illustrations of the time windows in which fragments of the ASE are active in development. Pink panels indicate pupal stage; green panels indicate adult stage; and red lines represent levels of Su(H) expression. *Su(H)* autoregulation is established in the pupal notum between 18 and 24 hr APF and persists into adulthood. The dashed vertical line marks the time (24 hr APF) when ASE5 is normally activated by an above-threshold level of Su(H); this threshold is indicated by the dashed horizontal line. In each illustration, the purple vertical line marks the suggested time (if ever) when the indicated *Su(H)* rescue transgene reaches the threshold required to activate ASE5.
See also Figures S5 and S6.
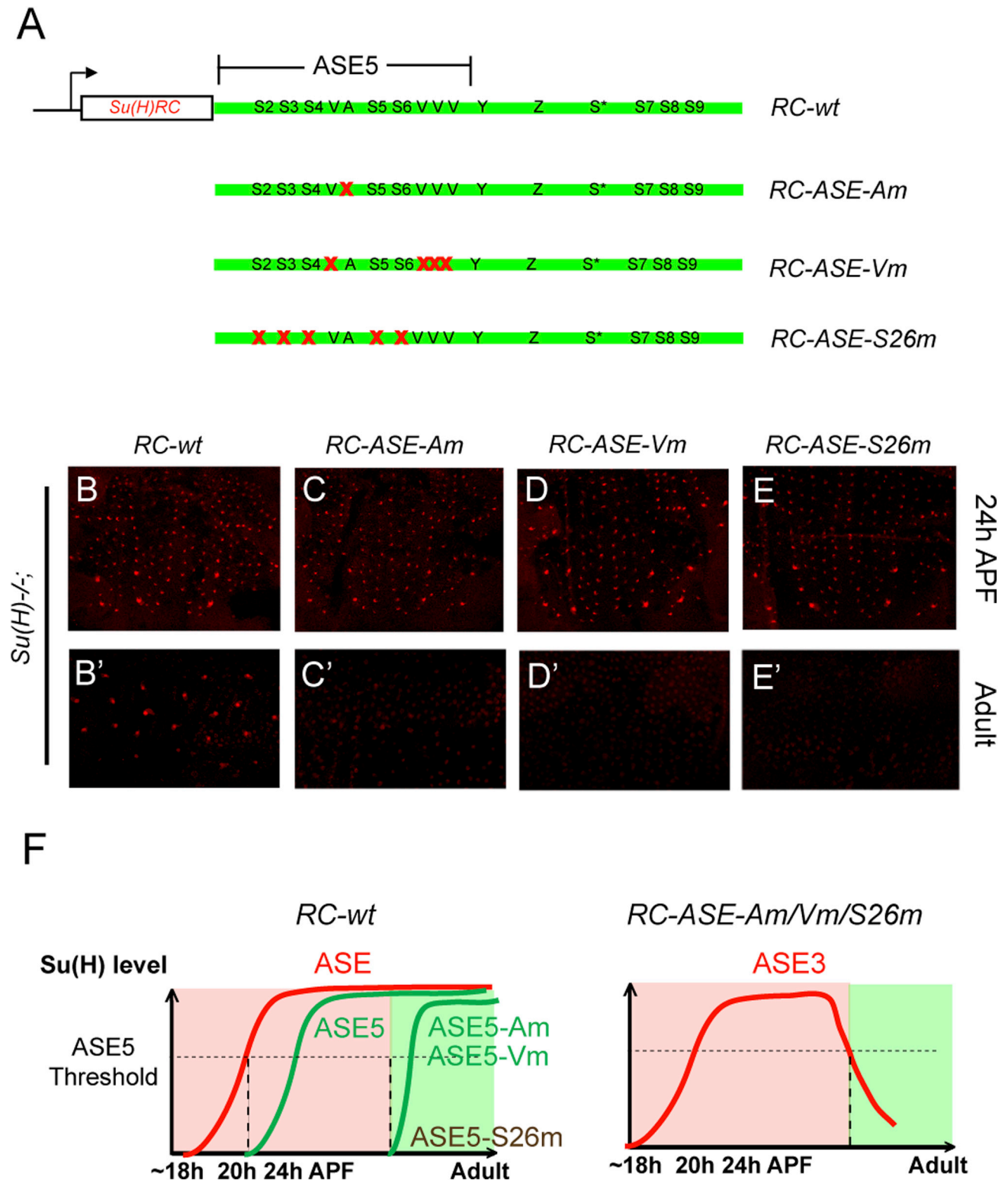
Figure 6. ASE5 Is Combinatorially Activated in Pupal Stages to Maintain *Su(H)* Autoregulation in Adults

(A) Diagrams of *Su(H)* rescue constructs carrying point mutations in the ASE5 submodule of the ASE. Note that the ASE5 region has been expanded out of proportion to the rest of the ASE in order to illustrate the sequence motif composition of ASE5. Red X's indicate mutated motifs.

(B–E) Anti-Su(H) antibody staining in the pupal notum at 24 hr APF. (B'–E') Anti-Su(H) antibody staining in the adult abdominal epithelium.

(F) (Left) Cartoon summary of the effects of mutating the A motif or the Vvl sites on the function of an *ASE5-GFP* reporter (green lines) in a wild-type background (Liu and Posakony, 2012). In the presence of normal levels of Su(H) (red line), ASE5 normally becomes active in the socket cell of the microchaetes in the pupal

(legend continued on next page)
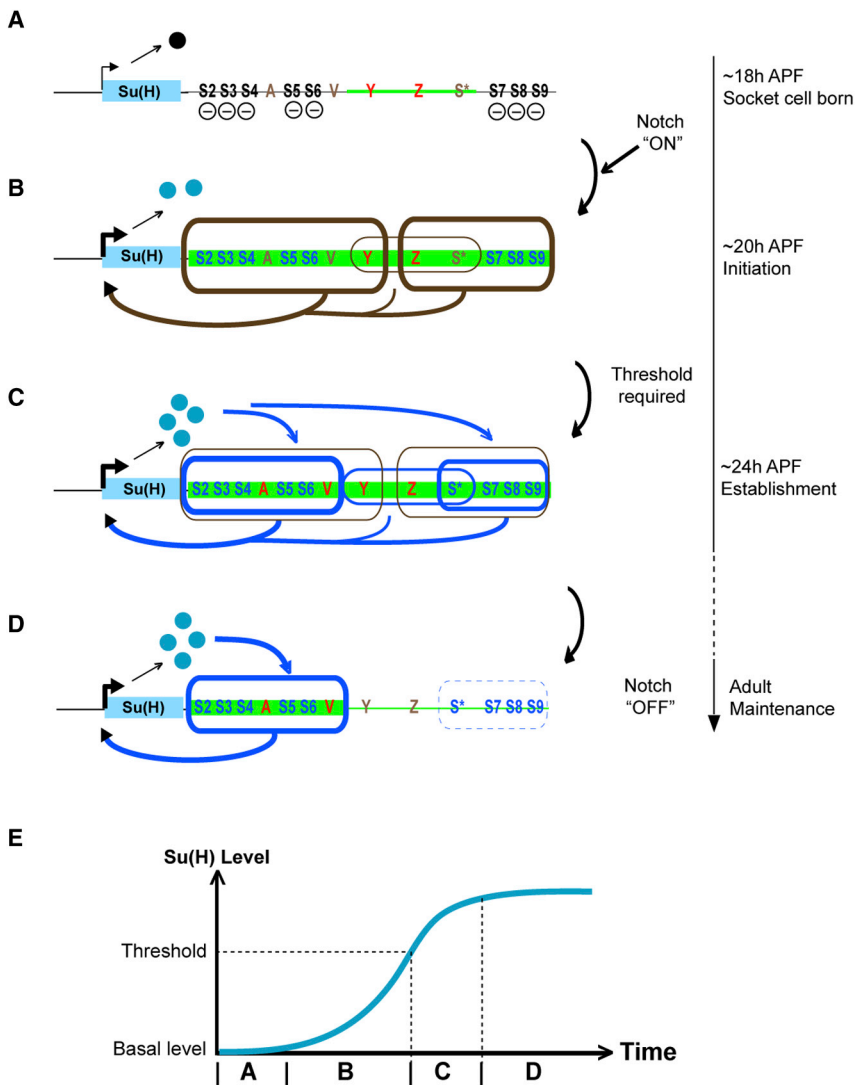
Figure 7. Model of How the ASE Integrates Multiple Feedback Loops to Control *Su(H)* Autoregulation in the Differentiating Socket Cell

(A–D) Diagrams depicting the dynamic interaction between the ASE and its functional inputs in the socket cell. The time line at right refers to the developmental stages of microchaete socket cells in the pupal notum. The body of the *Su(H)* gene is represented as a blue box; the accompanying arrow shows the direction of transcription, with its thickness denoting the intensity of transcriptional activity in the socket cell. The ASE is shown downstream of the gene, with functionally important sequence motifs and subregions labeled. Segments of the ASE receiving local activator inputs are highlighted in green, with the input level indicated by the thickness of the green line. The repressor form of Su(H) is shown as a black ball; the activator form is shown as blue balls.

(A) Shortly after the socket cell is born, the ASE receives local activator inputs via the sequences in YZW (thin green line, red Y and Z) but is silenced by the default repression function of Su(H), acting via binding sites S2–S9 (—).

(B) Activation of the Notch pathway in the socket cell converts Su(H) into a transcriptional activator (Barolo et al., 2000). Su(H) and various local activator inputs selectively synergize to activate two submodules, ASE5Y and ZW3S (brown boxes, thick lines), which drive an increase in *Su(H)* transcription (thick brown arrows). YZW (brown box, thin line) may also contribute independently to this activity (thin brown arrow).

(C) Once Su(H) expression rises above a threshold level, two Su(H) response elements, ASE5 and W3S (blue boxes, thick lines), are activated to fully establish the ASE-*Su(H)* feedback loop (blue arrows). Activation of ASE5 and W3S depends in part on other local activator inputs; in particular, ASE5 receives two activator inputs via a single A motif (red A) and multiple binding sites for Vvl (red V), a POU-homeodomain transcription factor (Liu and Posakony, 2012).

(D) As the socket cell differentiates, the local activator inputs on YZW disappear (brown Y and Z) and W3S is silenced (blue box, dashed line), but the activator inputs on ASE5 persist into adulthood, keeping ASE5 active to maintain *Su(H)* autoregulation (blue arrows). See also Figure S7.

(E) The dynamic pattern of activation of the ASE's submodules progressively establishes *Su(H)* autoregulation in the socket cell. Letters on the time axis refer to stages (A)–(D) above.

Finally, as the socket cell differentiates, the factors acting upon Y and Z disappear from the socket cell, leading to the inactivation of the three submodules—ASE5Y, YZW, and ZW3S—that are responsible for the initiation of *Su(H)* autoregulation. However, one of the Su(H) response elements, ASE5, remains strongly active and maintains the autoregulatory loop into adulthood (Figure 7D). The other Su(H) response element, W3S, is silent at this stage, evidently due to a late repression function of the adjacent sequences (see Figure S7).

Another important dynamic element is embodied in the above model. Su(H) is seen to play an essential role in all three phases of *Su(H)* autoregulation in the socket cell—initiation, establishment, and maintenance. In the first step, initiation, Su(H) is already present at its low basal level; here, it is fully dependent on Notch signaling, which converts it from a repressor to an activator (Figures 7A and 7B). But we have shown previously that, in the long-term maintenance phase (Figure 7D), when Su(H) is present at a high level in the socket cell, it acts independently of

notum between 20 and 24 hr APF; ASE5-Am and ASE5-Vm are not active until prepharate adult stages; and ASE5-S26m is silent throughout development. (Right) Based on these prior results, on those shown in Figures 4J–4K′, and on those shown in (B)–(E′), we suggest that Su(H) expression directed by *RC-ASE-Am*, *RC-ASE-Vm*, and *RC-ASE-S26m* is due to ASE3 (red line). Like *RC-ASE3* (see Figures 4J and 4J′), these constructs all generate very substantial levels of Su(H) in pupal stages (C–E), but this early expression is not maintained in adults (C′–E′). We suggest that this is because by the time ASE3 becomes inactive, ASE5 has not been activated in time (*RC-ASE-Am* and *RC-ASE-Vm*) or has not been activated at all (*RC-ASE-S26m*).

Notch, possibly employing a distinct coactivator (Barolo et al., 2000). Thus, the transition from low-level initiation to high-level maintenance in *Su(H)* autoregulation involves a transition from a Notch-dependent to a Notch-independent mode of action for Su(H) and the ASE.

The ASE Consists of Interlocking Enhancer Submodules

An enhancer module is typically defined as a discrete genomic fragment capable of driving a specific pattern of gene transcription (with respect to location, time, and level). Most studies of enhancer function have accordingly treated each such module as a unit and have focused on its integrative capacity; namely, the enhancer's ability to synthesize multiple transcription factor inputs, both positive and negative, into a single transcriptional output.

Our detailed functional analysis of the ASE has revealed a more complex picture that emphasizes enhancer substructure. We have found that different component fragments of the full ASE have distinct functional roles to play in the initiation, establishment, and maintenance of cell-type-specific *Su(H)* autoregulation. One might perhaps conceive of these component fragments as discrete enhancer modules themselves, but as we have shown, their boundaries often overlap (for example, ASE5 and W3S are respectively embedded within ASE5Y and ZW3S), and in any case they all help generate the same output—continuous, elevated expression of Su(H) in the socket cell. Therefore, we suggest that it is conceptually more useful to think of the ASE as a single enhancer composed of several enhancer submodules that are functionally distinct, but not clearly separable physically. In a highly dynamic manner (Figure 7), each submodule makes an important contribution to the overall spatial, temporal, and quantitative *cis*-regulatory activity of the full enhancer. Conversely, the ASE's architecture gives it the ability to integrate these multiple regulatory contributions into a stably progressing temporal pattern of Su(H) expression in the differentiating socket cell (Figure 7E), a context in which both the external stimuli and the internal gene expression profile undergo dramatic changes. Such a sophisticated integration capacity has been observed previously for the control of some genes by a cohort of separate enhancer modules (de-Leon and Davidson, 2010; Wahl et al., 2009; Yuh et al., 1998, 2001), but our study shows that even a single enhancer may employ this strategy using a compact set of submodules.

Finally, we suggest that dividing the ASE's various activities among multiple functionally connected, and partially redundant, submodules confers on the enhancer considerable evolutionary flexibility to fine-tune almost every aspect of its function (time, space, and level). The successive employment of distinct submodules allows the ASE's activity at different stages to be modified separately by mutational changes within individual submodules. Likewise, the partially redundant functions of the ASE5Y and ZW3S initiation submodules allow each to undergo separate changes in a context in which the ASE's activity is buffered by the other submodule.

Interlinked Positive Feedback Loops Create a Stable "Lockdown" Switch

A particularly notable feature of the ASE is that each of its submodules contains one or a few Su(H) binding sites. Because each submodule can activate *Su(H)* transcription independently, and at the same time can respond to direct activation by Su(H), the reciprocal interaction between the ASE and *Su(H)* comprises not one, but several, interlinked positive feedback loops (Figure 7). Furthermore, due in part to the requirement for different levels of Su(H) for sub-module activation, the feedback loops between the ASE and *Su(H)* are interlinked in three distinct layers. The first linkage occurs among the ASE's three initiation submodules (ASE5Y, YZW, and ZW3S), which cooperate to drive Su(H) expression above its basal level (Figure 7B). The second linkage is between the initiation submodules and the two Su(H) response elements (ASE5 and W3S), because the activities of the former group are responsible for generating the high level of Su(H) required to activate the latter (Figure 7C). The third linkage occurs between the two Su(H) response elements themselves: when they are activated by high levels of Su(H), each then acts as a discrete Su(H) autoregulatory enhancer to reinforce the other's activity via the feedback input from Su(H) (Figure 7C). The logic of this system is evident: once a certain threshold level of Su(H) expression is established by the linked initiation submodules of the ASE, it can be quickly "locked down" by the linked autoregulatory functions of the Su(H) response elements.

Recent studies have suggested that, in comparison with single positive feedback loops, interlinked positive feedback loops with different time constants are less sensitive to background noise and more effective at mediating rapid irreversible gene activation (Brandman et al., 2005). We suggest that the ASE represents a transcriptional implementation of this paradigm. For example, when the function of one of the ASE's initiation submodules is removed, *Su(H)* autoregulation can still be established, but the process is either fast-and-reversible (e.g., *RC-ASE3*) or slow-and-irreversible (e.g., *RC-ASE5Y*). Thus, whereas a simpler module might indeed be capable of establishing *Su(H)* autoregulation per se, the interlinked feedback loops of the ASE ensure that this happens rapidly and robustly, in a switch-like manner.

EXPERIMENTAL PROCEDURES

Plasmid Constructs

The sequences of the ASE, *Su(H) RC-wt*, and *Su(H) RC-ΔASE* were defined previously (Barolo et al., 2000). To make GFP reporter transgene constructs, the full ASE and its variants were amplified by PCR and cloned into the EcoRI and BamHI sites of the plasmid vector *pH-Stinger-attB* (Steven W. Miller, UCSD).

Su(H) rescue constructs were generated in three steps. First, the φC31 attB recognition sequence (Huang et al., 2009) was amplified by PCR and cloned into the HindIII site of the P element-based plasmid vector *pNot-CaSpeR* to generate the vector *attB-pNot-CaSpeR*. Second, the genomic DNA fragment *Su(H) RC-ΔASE* (Barolo et al., 2000) was amplified by PCR and cloned into the NotI and BamHI sites of the *attB-pNot-CaSpeR vector*. Third, the BamHI site in the *attB-pNot-CaSpeR/Su(H) RC-ΔASE* plasmid was used to insert the ASE or its variants to generate the rescue constructs described in this study. Only constructs containing inserts matching the orientation of the wild-type ASE with respect to the *Su(H)* coding sequences were used to generate transgenic flies.

Plasmid constructs were confirmed by DNA sequencing (GENEWIZ San Diego). PCR primers used for the above experiments are described in the Supplemental Experimental Procedures.

Drosophila Stocks and Crosses

Drosophila embryo injections were performed in accordance with standard protocols (Rubin and Spradling, 1982). Both the GFP reporter gene and

Su(H) rescue constructs were integrated into the attP2 docking site on the third chromosome (68A4) using the φC31 integrase system (Bischof et al., 2007). Transgenic lines were backcrossed to the *w^1118^* strain to establish homozygous stocks.

The flies used for *Su(H)* rescue experiments are of the following genotype: *Su(H)^AR9^/Su(H)^SF8^; p[w^+^; RC-ASE*]* (ASE* indicates the ASE or its variants). *Su(H)^AR9^* and *Su(H)^SF8^* are both null alleles (Schweisguth and Posakony, 1992). To assay GFP reporter gene expression in the Su(H)^low^ background, the following crosses were performed: *Su(H)^AR9^/Cyo, Kr > GFP; p[ASE*-GFP]* X *Su(H)^AR9^/Su(H)^SF8^; p[RC-ΔASE]*. Progeny of the genotype *Su(H)^AR9^/Su(H)^SF8^; p[RC-ΔASE]/p[ASE*-GFP]* were distinguished by the lack of *Kr>GFP* expression in the pupal trunk (Casso et al., 2000).

For the feedback transition assay, the following crosses were performed: *Su(H)^AR9^/Cyo, Kr > GFP; p[ASE5-GFP]* X *Su(H)^AR9^/Su(H)^SF8^; p[RC-ASE*]*. Progeny of the genotype *Su(H)^AR9^/Su(H)^SF8^; p[RC-ASE*]/ p[ASE5-GFP]* were distinguished by the lack of *Kr>GFP* expression in the pupal trunk (Casso et al., 2000).

All crosses were carried out at 25°C. For timed dissection, white prepupae (0 hr APF) were handpicked and cultured in a humidified chamber until the desired time point for dissection.

Immunohistochemistry and Confocal Microscopy

Pupal nota and adult abdominal epithelia were dissected in PBT (1XPBS, 0.1% Triton X-100) and fixed in 4% paraformaldehyde in 1XPBT for 30 min at room temperature. After three washes in PBT, tissues were used for direct visualization of GFP fluorescence or for immunohistochemistry. Primary antibodies used were Guinea pig anti-D-Pax2 polyclonal antibody (1:1,000; Steven W. Miller, UCSD), rabbit anti-GFP polyclonal antibody (1:1,000; Invitrogen), mouse anti-Prospero monoclonal antibody (1:10; Developmental Studies Hybridoma Bank) (Spana and Doe, 1995), and rabbit anti-Su(H) polyclonal antibody (1:1,000; Santa Cruz Biotechnology). Secondary antibodies used were anti-rabbit-Alexa488, anti-rabbit-Alexa555, anti-mouse-Alexa555, and anti-guinea pig-Alexa647, all diluted 1:200 (Molecular Probes).

Fluorescent images were collected with a Leica TCS SP2 confocal microscope (Leica Microsystems). Each image was generated as an average projection of a series of Z-section images taken at 2 μm intervals. All images were collected using the same magnification and gain settings. Care was taken to select representative images from each experiment, though little variation was apparent between repetitions. Experiments to be directly compared were conducted, and the results imaged, at the same time.

GFP levels were scored using the following semiquantitative system: strong, +++; moderate, ++; weak, +; weak stochastic, −/+; and negative, −.

REFERENCES

Bailey, A.M., and Posakony, J.W. (1995). Suppressor of hairless directly activates transcription of *enhancer of split complex* genes in response to Notch receptor activity. Genes Dev. *9*, 2609–2622.

Barolo, S., Walker, R.G., Polyanovsky, A.D., Freschi, G., Keil, T., and Posakony, J.W. (2000). A notch-independent activity of suppressor of hairless is required for normal mechanoreceptor physiology. Cell *103*, 957–969.

Bischof, J., Maeda, R.K., Hediger, M., Karch, F., and Basler, K. (2007). An optimized transgenesis system for *Drosophila* using germ-line-specific phiC31 integrases. Proc. Natl. Acad. Sci. USA *104*, 3312–3317.

Brandman, O., Ferrell, J.E.J., Jr., Li, R., and Meyer, T. (2005). Interlinked fast and slow positive feedback loops drive reliable cell decisions. Science *310*, 496–498.

Casso, D., Ramírez-Weber, F., and Kornberg, T.B. (2000). GFP-tagged balancer chromosomes for *Drosophila melanogaster*. Mech. Dev. *91*, 451–454.

Crews, S.T., and Pearson, J.C. (2009). Transcriptional autoregulation in development. Curr. Biol. *19*, R241–R246.

de-Leon, S.B., and Davidson, E.H. (2010). Information processing at the foxa node of the sea urchin endomesoderm specification network. Proc. Natl. Acad. Sci. USA *107*, 10103–10108.

Fortini, M.E., and Artavanis-Tsakonas, S. (1994). The suppressor of hairless protein participates in notch receptor signaling. Cell *79*, 273–282.

Hobert, O. (2011a). Regulation of terminal differentiation programs in the nervous system. Annu. Rev. Cell Dev. Biol. *27*, 681–696.

Hobert, O. (2011b). Maintaining a memory by transcriptional autoregulation. Curr. Biol. *21*, R146–R147.

Huang, J., Zhou, W., Dong, W., and Hong, Y. (2009). Targeted engineering of the Drosophila genome. Fly (Austin) *3*, 274–277.

Kavaler, J., Fu, W., Duan, H., Noll, M., and Posakony, J.W. (1999). An essential role for the Drosophila Pax2 homolog in the differentiation of adult sensory organs. Development *126*, 2261–2272.

Liu, F., and Posakony, J.W. (2012). Role of architecture in the function and specificity of two Notch-regulated transcriptional enhancer modules. PLoS Genet. *8*, e1002796.

Miller, S.W., Avidor-Reiss, T., Polyanovsky, A., and Posakony, J.W. (2009). Complex interplay of three transcription factors in controlling the tormogen differentiation program of *Drosophila* mechanoreceptors. Dev. Biol. *329*, 386–399.

Nellesen, D.T., Lai, E.C., and Posakony, J.W. (1999). Discrete enhancer elements mediate selective responsiveness of *enhancer of split* complex genes to common transcriptional activators. Dev. Biol. *213*, 33–53.

Richards, G.S., and Degnan, B.M. (2012). The expression of Delta ligands in the sponge Amphimedon queenslandica suggests an ancient role for Notch signaling in metazoan development. Evodevo *3*, 15.

Rubin, G.M., and Spradling, A.C. (1982). Genetic transformation of *Drosophila* with transposable element vectors. Science *218*, 348–353.

Schweisguth, F., and Posakony, J.W. (1992). Suppressor of Hairless, the Drosophila homolog of the mouse recombination signal-binding protein gene, controls sensory organ cell fates. Cell *69*, 1199–1212.

Spana, E.P., and Doe, C.Q. (1995). The prospero transcription factor is asymmetrically localized to the cell cortex during neuroblast mitosis in *Drosophila*. Development *121*, 3187–3195.

Tun, T., Hamaguchi, Y., Matsunami, N., Furukawa, T., Honjo, T., and Kawaichi, M. (1994). Recognition sequence of a highly conserved DNA binding protein RBP-J kappa. Nucleic Acids Res. *22*, 965–971.

Wahl, M.E., Hahn, J., Gora, K., Davidson, E.H., and Oliveri, P. (2009). The *cis*-regulatory system of the tbrain gene: alternative use of multiple modules to promote skeletogenic expression in the sea urchin embryo. Dev. Biol. *335*, 428–441.

Yuh, C.H., Bolouri, H., and Davidson, E.H. (1998). Genomic *cis*-regulatory logic: experimental and computational analysis of a sea urchin gene. Science *279*, 1896–1902.

Yuh, C.H., Bolouri, H., and Davidson, E.H. (2001). *cis*-regulatory logic in the endo16 gene: switching from a specification to a differentiation mode of control. Development *128*, 617–629.